10th World Congress on Structural and Multidisciplinary Optimization
May 19 - 24, 2013, Orlando, Florida, USA

Solving multiobjective optimization problems using quasi-separable MDO formulations and analytical target cascading

Namwoo Kang[1], Michael Kokkolaras[2], Panos Y. Papalambros[1]

[1]University of Michigan, Ann Arbor, MI, USA, {nwkang, pyp}@umich.edu
[2]McGill University, Montreal, QC, Canada, michael.kokkolaras@mcgill.ca

1. Abstract
An approach to multiobjective optimization is to define a scalar substitute objective function that aggregates all objectives and solve the resulting aggregate optimization problem (AOP). In this paper, we discern that the objective function in quasi-separable multidisciplinary design optimization (MDO) problems can be viewed as such an aggregate objective function (AOF). We consequently claim that a method that can solve quasi-separable problems can also be used to obtain Pareto points of associated AOPs. Our motivation stems from cases where AOPs are too hard to solve or when the design engineer does not have access to the models necessary to evaluate all the terms of the AOF . In this case, decomposition-based design optimization methods can be particularly useful to solve the AOP as a quasi-separable MDO problem. Specifically, we use the analytical target cascading methodology to formulate decomposed subproblems of quasi-separable MDO problems and coordinate their solution in order to obtain Pareto points of the associated AOPs. We first illustrate our approach using a well-known simple geometric programming example and then present a vehicle suspension design problem with three objectives related to ground vehicle ride and handling.

2. Keywords: Multiobjective optimization, quasi-separable MDO problems, analytical target cascading

3. Introduction
An approach to solving multiobjective optimization (MO) problems is to define a scalar substitute objective function that aggregates the components of the vector of objectives. This aggregate objective function (AOF) includes weight parameters so that the Pareto set of the original MO problem can be populated by solving the single-objective optimization problem for different values of these parameters.

A popular and widely-used technique that follows this approach is to define a weighted sum of the objectives and vary the weights to obtain different Pareto points. Oftentimes, the weights are required to sum up to 1, but this is not strictly necessary. It is also well known that linear combinations of the objectives may miss points on non-convex parts of Pareto sets [1]. These issues are not addressed here.

In this paper we consider MO problems in the design of large, complex engineering systems, where some of the objectives may not be under the control of the design engineer. For example, the system designer may not have access to the modeling and simulation models that evaluate these objectives because the analysis model may have been either distributed to subject matter experts or outsourced. Such situations are typical in multidisciplinary design optimization (MDO) problems, whose formulations are used to implement decomposition-based optimization strategies.

The main idea investigated in this paper is based on the observation that the objective function of quasi-separable MDO problems [2, 3] can be viewed as a weighted sum of competing objectives of an MO problem with equal weights. Further, we assume that the use of MDO methodologies is required because the MO problem cannot be solved using an all-in-one approach. In this context, we propose solving the multiobjective optimization problem formulated as a quasi-separable MDO one using analytical target cascading (ATC) [4]. Specifically, we decompose the AOF by formulating a subproblem for each objective and use non-hierarchical ATC [5] to coordinate the solution of the decomposed problem.

The article is organized as follows. The proposed methodology is presented in Section 4. In Section 5, we use a simple geometric programming problem that can be viewed as a bi-objective problem to illustrate the proposed methodology. A more complex elaborate vehicle suspension design problem for optimizing ground vehicle ride and handling quality by considering multiple objectives for ride comfort, controllability and stability is presented in Section 6. Summarizing remarks are made in Section 7.

4. Solving MO problems using quasi-separable MDO formulation and ATC

The general MO problem is formulated as

$$\begin{array}{ll} \min\limits_{\mathbf{x}} & \mathbf{f} = [f_1(\mathbf{x}), f_2(\mathbf{x}), \ldots, f_N(\mathbf{x})] \\ \text{subject to} & \mathbf{g}(\mathbf{x}) \leq \mathbf{0} \\ & \mathbf{h}(\mathbf{x}) = \mathbf{0}. \end{array} \tag{1}$$

Note that the vector $\mathbf{x}$ represents a collection of all the variables that appear in all the functions of the MO problem and that vectors are assumed to be row vectors to avoid repeated use of transpose symbols. In reality, not all functions will depend on all of the variables in the vector $\mathbf{x}$; each function usually depends only on a subset of the variables included in the vector $\mathbf{x}$. The basic assumption is that every pair of objective functions will depend on at least one common variable; otherwise the problem can be completely or partially separated.

Let the subset of the variables included in $\mathbf{x}$, on which the j-th objective function depends, be denoted by $\hat{\mathbf{x}}_j = [\mathbf{y}, \mathbf{x}_j]$. Then the MO problem is reformulated as in Eq. (2):

$$\begin{array}{ll} \min\limits_{\mathbf{y}, \mathbf{x}_j, \ldots, \mathbf{x}_N} & \sum_{j=1}^{N} w_j f_j(\mathbf{y}, \mathbf{x}_j) \\ \text{subject to} & \mathbf{g}_j(\boldsymbol{y}, \mathbf{x}_j) \leq \mathbf{0} \quad j = 1, \ldots, N \\ & \mathbf{h}_j(\boldsymbol{y}, \mathbf{x}_j) = \mathbf{0} \quad j = 1, \ldots, N \end{array} \tag{2}$$

The AOF is defined by a weighted sum, where f_j denotes the j-th objective function and w_j is the associated weight ($j = 1, \ldots, N$). For simplicity and without loss of generality, we assume that all objective functions share the same number of variables $\mathbf{y}$ (the contrary merely makes bookkeeping and notation more tedious), while $\mathbf{x}_j$ denotes the "local" variables that only the j-th objective function depends on. The equality and inequality constraints of the MO problem can be separated according to local design variables. Again, for simplicity and without loss of generality, we assume that there exists at least one inequality and one equality constraint that depend on local design variables $\mathbf{x}_j$ and that they both depend on the same number of shared variables $\mathbf{y}$.

The weighted sum formulation of the MO problem shown in Eq. (2) is identical to the quasi-separable MDO problem considered by Tosserams et al. in [3] if all the weights are set equal to 1. Therefore, the solution of a quasi-separable MDO problem is equivalent to the Pareto solution of the MO problem when all the weights are equal. Strictly speaking, the weighted sum method requires all the weights to sum up to 1; however, solving the MO problem with $w_j = 1 \; \forall \; j$ is equivalent to solving the MO problem with $w_j = 1/N \; \forall \; j$. Decomposition-based methodologies for MDO problems are motivated by the same reasons as for investigating decomposition-based approaches for MO: Either inability to solve the problem as "all-in-one" (AIO), or lack of control of some of the subproblems or disciplines involved. When the problem is decomposed, local variables that are copies of the shared variables are introduced into every subproblem and consistency constraints are formulated to ensure that all copies of shared variables are equal at feasible solutions. The functional dependence tables (FDT) of the AIO and decomposed problems are shown in Figure. 1 to illustrate the degree of separability of the two problem formulations.

(a) AIO problem

	$\mathbf{y}$	$\mathbf{x}_1$	$\mathbf{x}_2$	$\mathbf{x}_3$
$f_1\,\mathbf{g}_1\,\mathbf{h}_1$	•	•		
$f_2\,\mathbf{g}_2\,\mathbf{h}_2$	•		•	
$f_3\,\mathbf{g}_3\,\mathbf{h}_3$	•			•

(b) Decomposed problem

	$\mathbf{y}_1$	$\mathbf{x}_1$	$\mathbf{y}_2$	$\mathbf{x}_2$	$\mathbf{y}_3$	$\mathbf{x}_3$
$f_1\,\mathbf{g}_1\,\mathbf{h}_1$	•	•				
$f_2\,\mathbf{g}_2\,\mathbf{h}_2$			•	•		
$f_3\,\mathbf{g}_3\,\mathbf{h}_3$					•	•

Figure 1: Functional dependence tables for the AIO and decomposed problem formulations

Tosserams, Etman and Rooda proposed a bi-level decomposition of the quasi-separable MDO problem that uses a master problem at the top level to coordinate the consistency constraints [3]. Figure. 2 depicts an MO example with three objectives that is treated as a quasi-separable MDO problem with three subproblems. The non-hierarchical analytical target cascading formulation [5] enables us to solve the decomposed problem without the necessity of a master problem: The proposed methodology coordinates the auxiliary copies of the shared variables y_1, y_2 and y_3 directly among subproblems using penalty functions, eliminating the need to coordinate each auxiliary copy of the shared variables separately.

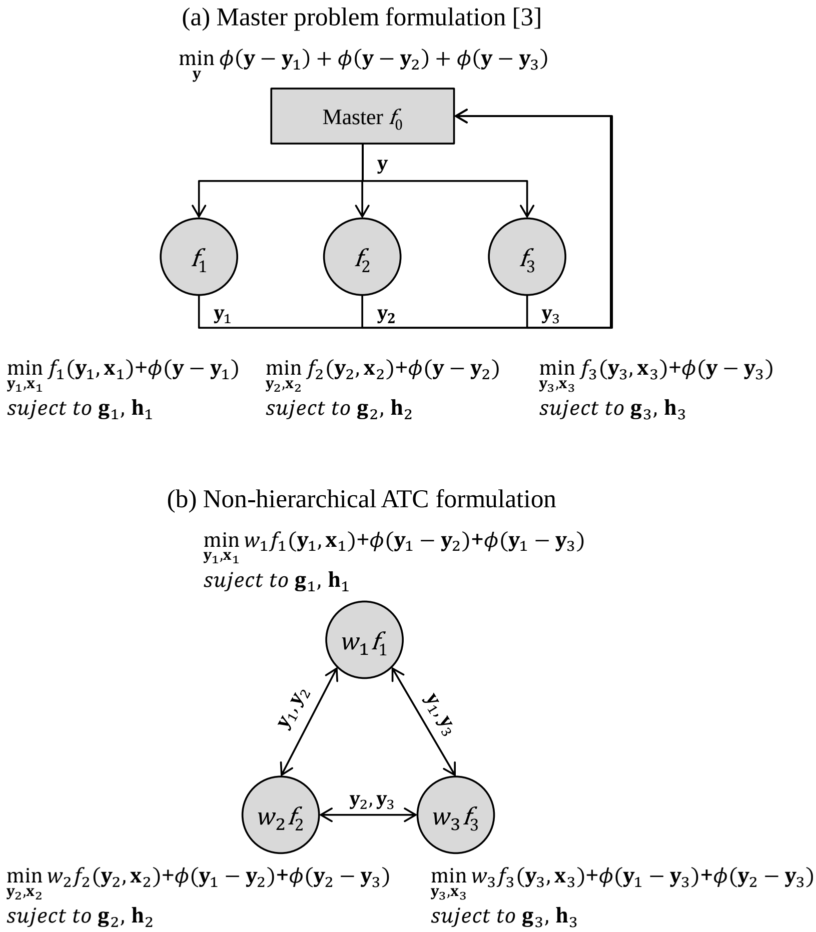

Figure 2: Solving MO problems using quasi-separable MDO formulations

Using the Augmented Lagrangian Penalty Function approach of [6], the general formulation for each subproblem is given in Eq. (3):

$$
\begin{array}{ll}
\min\limits_{\mathbf{y}_j,\mathbf{x}_j} & w_j f_j(\mathbf{y}_j,\mathbf{x}_j) + \sum_{i\neq j}^{N} \phi(\mathbf{y}_j-\mathbf{y}_i) \\
\text{subject to} & \mathbf{g}_j(\boldsymbol{y}_j,\mathbf{x}_j) \leq \mathbf{0} \\
 & \mathbf{h}_j(\boldsymbol{y}_j,\mathbf{x}_j) = \mathbf{0} \\
\text{with} & \phi(\mathbf{y}_j-\mathbf{y}_i) = \mathbf{v}_{ij}(\mathbf{y}_j-\mathbf{y}_i)^{\mathrm{T}} + \|\mathbf{w}_{ij}\circ(\mathbf{y}_j-\mathbf{y}_i)\|_2^2.
\end{array}
\tag{3}
$$

Here $\mathbf{v}_i$ is the vector of Lagrange multipliers, $\mathbf{w}_i$ is the vector of penalty weights, and the Hadamard symbol $\circ$ is used to denote term-by-term multiplication of vectors. The iterative coordination algorithm used here is the method of multipliers as outlined in [5]: At every iteration q we solve all subproblems (in any sequence or in parallel), and then update the penalty weights according to

$$
w_{ij,k}^{q+1} = \begin{cases} w_{ij,k}^{q} & \text{if} \quad |(y_{j,k}-y_{i,k})^q| \leq \gamma|(y_{j,k}-y_{i,k})^{q-1}| \\ \beta w_{ij,k}^{q} & \text{if} \quad |(y_{j,k}-y_{i,k})^q| > \gamma|(y_{j,k}-y_{i,k})^{q-1}| \end{cases}, \tag{4}
$$

where the subscript k denotes vector components. It is recommended that $\beta > 1$ and $0 < \gamma < 1$; we have used $\beta = 1.25$ and $\gamma = 0.4$ in the examples below. The Lagrange multipliers are then updated using

$$
\mathbf{v}_{ij}^{q+1} = \mathbf{v}_{ij}^{q} + 2\ \mathbf{w}_{ij}^{q}\circ\mathbf{w}_{ij}^{q}\circ(\mathbf{y}_j-\mathbf{y}_i)^q. \tag{5}
$$

The iterative coordination algorithm is terminated when both of two conditions are satisfied. Let us denote the collection of all consistency constraints $(\mathbf{y}_j-\mathbf{y}_i)\ \forall\ j$ and i by a vector $\mathbf{c}$. The first condition requires that the change in the maximal consistency constraint value after two consecutive iterations is smaller than a user-specified small positive threshold ε_1:

$$
\|\mathbf{c}^{\mathbf{k}}-\mathbf{c}^{\mathbf{k-1}}\|_\infty < \varepsilon_{\mathbf{1}}. \tag{6}
$$

The second condition requires that the maximal consistency constraint violation is smaller than a user-specified small positive threshold ε_2

$$\|\mathbf{c^k}\|_\infty < \varepsilon_\mathbf{2}. \tag{7}$$

Note that the decomposed problem can be solved with different weights to obtain different Pareto solutions of the MO problem. As mentioned before, possible non-convex parts of Pareto sets may not be generated since the quasi-separable MDO formulation is a linear combination of objective functions.

5. Illustration example

We apply the proposed method to a reduced version of the geometric programming problem, originally proposed in [4] and [7], and used in [3]:

$$\begin{array}{ll} \min\limits_{z_1,z_2,\ldots,z_7} & f = z_1^2 + z_2^2 \\ \text{subject to} & g_1 = (z_3^{-2} + z_4^2) - z_5^2 \leq 0 \\ & g_2 = (z_5^2 + z_6^{-2}) - z_7^2 \leq 0 \\ & h_1 = z_1^2 - (z_3^2 + z_4^{-2} + z_5^2) = 0 \\ & h_2 = z_2^2 - (z_5^2 + z_6^2 + z_7^2) = 0 \\ & [z_1, z_2, z_3, z_4, z_5, z_6, z_7] \geq \mathbf{0} \end{array} \tag{8}$$

From a mathematical perspective, the equality constraints can obviously be used to reduce the size of the problem. In our case, we use the equality constraints to define two objective functions, add weights and view the problem as an MO:

$$\begin{array}{ll} \min\limits_{z_3,z_4,z_5,z_6,z_7} & f = w_1 f_1(z_3, z_4, z_5) + w_2 f_2(z_5, z_6, z_7) \\ \text{subject to} & g_1 = (z_3^{-2} + z_4^2) - z_5^2 \leq 0 \\ & g_2 = (z_5^2 + z_6^{-2}) - z_7^2 \leq 0 \\ & [z_3, z_4, z_5, z_6, z_7] \geq \mathbf{0} \\ \text{with} & f_1 = z_3^2 + z_4^{-2} + z_5^2 \\ \text{and} & f_2 = z_5^2 + z_6^2 + z_7^2. \end{array} \tag{9}$$

We first solve the problem in Eq. (8) using an AIO approach. Then the problem in Eq. (9) is decomposed into two subproblems as shown in Figure 3, and solved using ATC. Note that the constraints are decomposed as mentioned above, i.e., by local design variables.

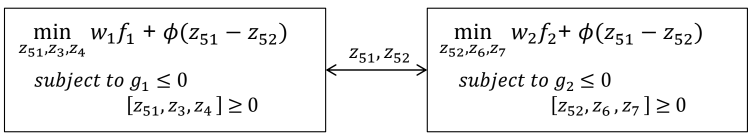

Figure 3: Decomposition of the problem in Eq. (9)

The two problems share variable z_5; we thus introduce auxiliary copies z_{51} and z_{52} to Subproblems 1 and 2, respectively, to replace the shared variable z_5. Matlab's implementation of the Sequential Quadratic Programming (SQP) algorithm (Matlab function `fmincon`) [8] is used to solve both the AIO and the decomposed problems. Figure. 4(a) and Figure. 4(b) shows the Pareto solutions obtained for several sets of weights for the problem in Eg. (8) and Eq. (9) respectively. Note that we have not used weights that sum up to one; we are using weight ratios to emphasize one objective. For example, the second solution emphasizes objective f_2 4 times more than objective f_1; this is equivalent to using weights 0.2 and 0.8 in the weighted sum method where the weights have to add up to 1.

The obtained results demonstrate that we can successfully solve the MO problem as a quasi-separable MDO problem using decomposition and non-hierarchical ATC coordination. We will now present a more elaborate design problem that motivates the use of their method in engineering design applications where the design engineer may not be able to solve the MO problem using an AIO approach.

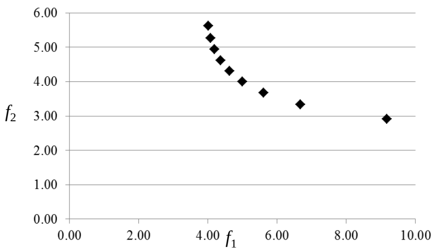

Weight		Optimal values						
w_1	w_2	f_1	f_2	z_3	z_4	z_5	z_6	z_7
1.0	9.0	9.18	2.92	2.09	0.48	0.68	1.00	1.21
1.0	4.0	6.67	3.33	1.73	0.58	0.82	1.00	1.29
1.0	2.3	5.60	3.68	1.54	0.65	0.92	1.00	1.36
1.0	1.5	5.00	4.00	1.41	0.71	1.00	1.00	1.41
1.0	1.0	4.62	4.31	1.32	0.76	1.07	1.00	1.47
1.5	1.0	4.36	4.62	1.24	0.81	1.14	1.00	1.52
2.3	1.0	4.19	4.94	1.17	0.86	1.21	1.00	1.57
4.0	1.0	4.08	5.27	1.11	0.90	1.28	1.00	1.62
9.0	1.0	4.02	5.62	1.05	0.95	1.35	1.00	1.68

(a) AIO problem

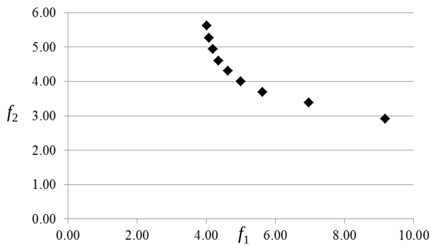

Weight		Optimal values						
w_1	w_2	f_1	f_2	z_3	z_4	z_5	z_6	z_7
1.0	9.0	9.18	2.92	2.09	0.48	0.68	1.00	1.21
1.0	4.0	6.96	3.38	1.77	0.56	0.82	1.00	1.31
1.0	2.3	5.62	3.68	1.55	0.65	0.92	1.00	1.36
1.0	1.5	4.99	4.00	1.41	0.71	1.00	1.00	1.41
1.0	1.0	4.62	4.31	1.32	0.76	1.07	1.00	1.47
1.5	1.0	4.35	4.60	1.23	0.81	1.14	1.00	1.52
2.3	1.0	4.19	4.94	1.17	0.86	1.21	1.00	1.57
4.0	1.0	4.08	5.27	1.11	0.90	1.28	1.00	1.62
9.0	1.0	4.02	5.62	1.05	0.95	1.34	1.00	1.68

(b) Decomposed problem

Figure 4: Pareto solutions for the modified geometric programming problem

6. Vehicle suspension design

6.1. Problem definition and simulation models

The problem involved a suspension design application for commercial vans considering ride and handling (R&H) quality. In general, R&H quality cannot be defined by a single aspect or attribute because it represents a complex qualitative "feeling" of the driver. It can be quantified in part using vehicle dynamic characteristics depending on driving situations. In this study, R&H quality is expressed through three objectives, ride comfort, controllability, and stability; three representative vehicle test methods are used to quantify each objective, as shown in Table 1.

Table 1: Design objectives and associated tests

Objective	Test	Description of test
Ride comfort	Bumpy ride test [9]	Measure the acceleration signal at the driver seat position at the moment of driving over bump
Stability	On-Centre handling test [10]	Measure yaw rate for the steering feel and precision of a vehicle during nominally straight-line driving and in negotiating large radius bends at high speeds but low lateral acceleration
Controll-ability	Roll control test on cornering [11]	Measure damping of roll movement with step steer input at constant speed and wide range of lateral accelerations

To incorporate these vehicle test methods into simulation and analysis models for optimization, the models for two levels (i.e., vehicle and suspension system levels) are built as shown in Figures 5 and 6. At the vehicle level, the simulation models to test the vehicle are built using CarSim software [12] and analysis models for test results are implemented in Matlab, as in Figure 5. The three vehicle simulation models have kinematic and compliance (K&C) characteristics as inputs decided by the suspension system design. These characteristics will be explained below at the system level discussion. The simulation models generate vehicle movements such as acceleration, yaw rate, and roll. Analysis models to translate the simulation results into R&H quality follow the international standards of quantification methods published from the international organization for standardization (ISO) [9, 10, 11]. For ride comfort, the bumpy ride simulation model generates body vertical accelerations with time, and we obtain peak-to peak amplitude from the wave graph with time as x-axis and body vertical accelerations as y-axis. The larger the amplitude is, the more impact drivers can feel when driving over a bump, and this magnitude of amplitude can be interpreted as a measure of vehicle ride comfort. For stability, the on-centre handling simulation model generates yaw rates with steering wheel angles, and these values show hysteresis loops with steering wheel angles as x-axis and yaw rates as y-axis. We obtain the horizontal width of the hysteresis loops at ordinate zero. The smaller the horizontal width is, the more sensitive is

the vehicle reaction. This magnitude of sensitivity can be interpreted as a measure of vehicle stability. For controllability, the roll control simulation model generates steady-state roll angles and peak roll angles with step steer inputs. We obtain the gradient of the linear function with steady-state roll angles (i.e., average roll angles at each step steer input) as x-axis, and peak roll angles as y-axis. A larger gradient represents a larger lurch of the vehicle. The magnitude of gradient can be then interpreted as a measure of vehicle roll controllability.
There is a challenge in how to decide the target value for each objective. Since the magnitudes of outputs are related to the feelings of drivers, they cannot be simply maximized or minimized as other objective metrics. In our formulation, target values are set for these objectives based on test data from existing vehicles that have been reported to have good reputation regarding R&H quality in the market place.

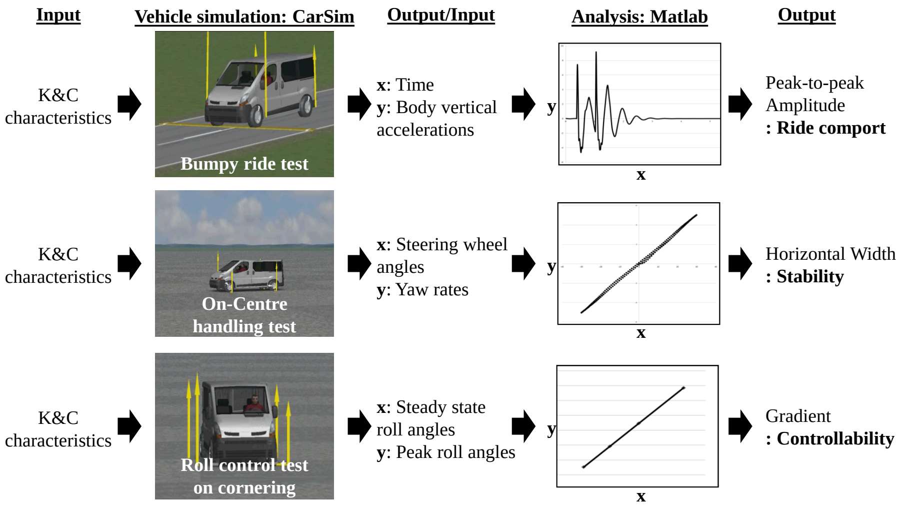

Figure 5: Simulation and analysis models at the vehicle level

At the suspension system level, the simulation model is built using MotionSolve software [13], as in Figure 6. Suspension design variables such as hard points, bushing stiffness, damper, and stabilizer bar stiffness are used as inputs. The outputs are six main K&C characteristics, left and right side of toe angle, camber angle, and front wheel longitudinal position. These K&C characteristics link the simulation models of vehicle and suspension system, and we can see how the design variables of the suspension system affect R&H quality of the vehicle. Kinematic characteristics are represented by the relative motion of joined system elements such as lower control arm, outer tie rod, knuckle, etc. Compliance characteristics are based on observing displacements of bush, spring and stabilizer bar elements. From analysis of K&C characteristics, a suspension designer can decide the hard point and stiffness of elements.
However, the K&C characteristic cannot be used directly as design optimization variables at the vehicle level because they are not defined by a single-valued variable but by non-linear functional relationships. The K&C characteristics can be represented by quadratic curves (i.e., $y = c_0 + c_1 x + c_2 x^2$) with respect to suspension characteristics such as camber, toe, caster, wheel position and wheel travel [14]. Therefore, the coefficients of quadratic curves (c_0, c_1, c_2) are used as design variables for the K&C characteristics. The feeling of ride comfort is very sensitive to the form of the K&C curve and the corresponding value of the ride comfort metric used as objective target. This will be discussed further in the optimization results.

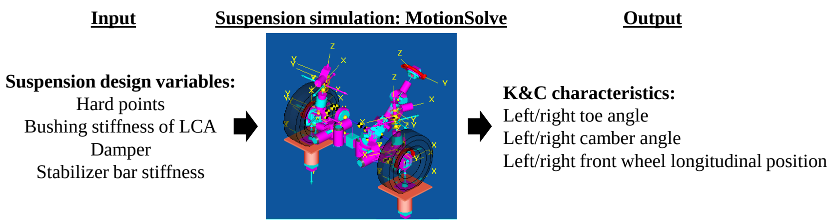

Figure 6: Simulation models at the suspension system level

6.2. ATC formulation

Previous research on ATC application to suspension system design [15, 16] did not consider R&H quality. Kang et al. addressed suspension design for R&H quality using a target cascading formulation [14], but without full coordination to achieve convergence between targets and responses. The present decomposition framework and detailed nomenclature are given in Figure 7 and Table 2, respectively. This framework is a combination of hierarchical and non-hierarchical ATC. Three subproblems (see f_1, f_2, and f_3 in Figure 7) have the same bi-level structure with vehicle level and system level as explained above. At the vehicle level, coefficients of K&C curves are cascaded to the system level as targets. At the system level, the optimal hard points and bushing stiffness of the suspension system are calculated to satisfy the target coefficients of K&C curves from the vehicle level. All suspension levels share the suspension design variables in the non-hierarchical structure as shown in Figure 2(b), and these shared variables $[\mathbf{y}_1, \mathbf{y}_2, \mathbf{y}_3]$ converge to a single optimal value. An SQP algorithm is used for solving each optimization problem. Each subproblem has six types of K&C curves which include three coefficients c_0, c_1, c_2. Therefore, for each subproblem, 18 coefficients are cascaded to the system level as targets from the vehicle level. The entire problem has total 108 design variables, with 54 design variables at the vehicle level (i.e., 3 coefficients $\times$ 6 curves $\times$ 3 subproblems) and 54 design variables at the system level (i.e., 18 shared design variables $\times$ 3 subproblems).

The first subproblem for ride comport at the vehicle level is stated in Eq. (10). The lower and upper bounds of the coefficients of the K&C curves were determined based on possible ranges given constraints on the suspension design variables. Response R_1 is obtained using the vehicle simulation and analysis model. Superscripts $(\cdot)^U$ and $(\cdot)^L$ indicate variables at the vehicle and system levels, respectively. To satisfy the target values obtained at the vehicle level, the design problem for suspension is formulated as in Eq. (11). The lower and upper bounds of the shared design variables were determined by considering the feasible design space of current van design parameters. Coefficients for the K&C curves C_1^L are obtained using the suspension simulation model shown in Figure 6.

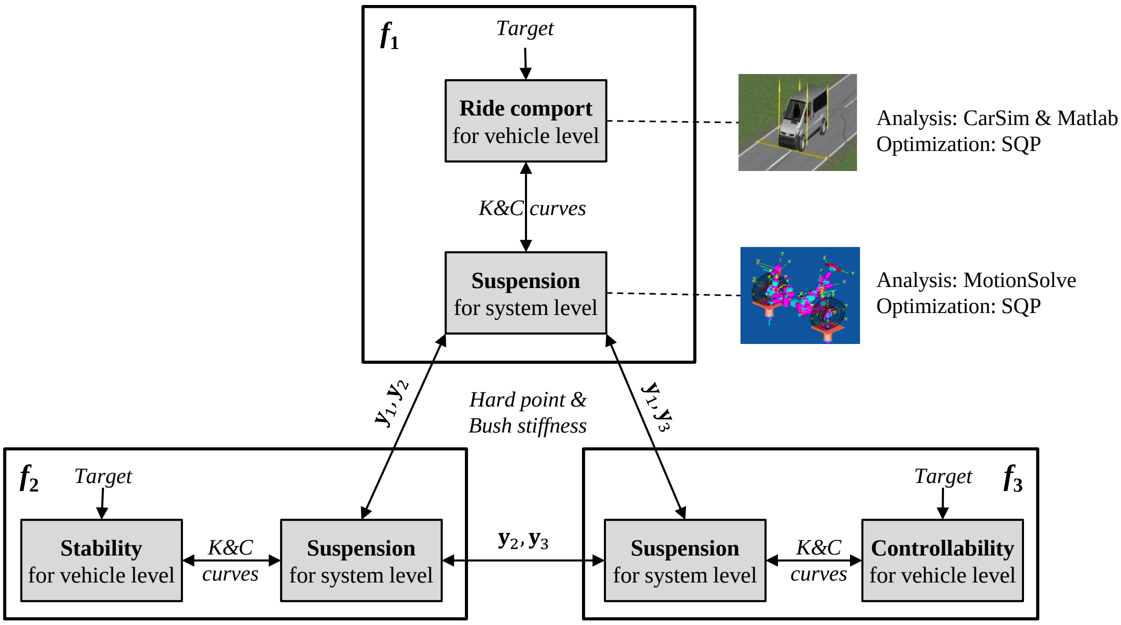

Figure 7: Decomposition and information flow of the non-hierarchical ATC

$$\begin{aligned} \min_{\mathbf{C}_1^U} \quad & \|T_1 - R_1\|_2^2 + \phi(\mathbf{C}_1^U - \mathbf{C}_1^L) \\ \text{subject to} \quad & lb \le \mathbf{C}_1^U \le ub \\ \text{where} \quad & R_1 = f_1(\mathbf{C}_1^U) \end{aligned} \tag{10}$$

$$\begin{aligned} \min_{\mathbf{y}_1} \quad & \phi(\mathbf{C}_1^U - \mathbf{C}_1^L) + \phi(\mathbf{y}_1 - \mathbf{y}_2) + \phi(\mathbf{y}_1 - \mathbf{y}_3) \\ \text{subject to} \quad & lb \le \mathbf{y}_1 \le ub \\ \text{where} \quad & \mathbf{C}_1^L = f_c(\mathbf{y}_1) \end{aligned} \tag{11}$$

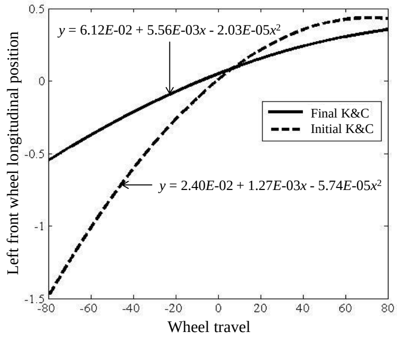

Figure 8: Example of K&C quadratic curve

Table 2: Targets, responses, and variables for the suspension design problem

Level	Variables and parameters
Vehicle level	**Targets** T_i: Target of i-th subproblem (i = 1: ride comfort, 2: stability, 3: controllability) **Responses** R_i: Response of i-th subproblem **Linking variables between vehicle and system levels (K&C curves)** C_{ijk}: Coefficient of k-th order of j-th K&C curve for i-th subproblem) (j = 1, 2, 3, 4, 5, 6) (k = 0, 1, 2)
System level	**Shared design variables among subproblems (suspension design variables)** $y_{ijk,hp}$: Coordinate of j-th axis of k-th hard point for i-th subproblem (j = 1: x-axis, 2: y-axis, 3: z-axis)(k = 1: LCA front bush, 2: LCA rear bush, 3: outer tie rod, 4: lower knuckle mounting) $y_{ijk,bs}$: Bush stiffness of j-th axis of k-th lower control arm (LCA) for i-th subproblem (j = 1: radial, 2: axial, 3: conical)(k = 1: front, 2: rear) $y_{i,d}$: Damper for i-th subproblem $y_{i,s}$: Stabilizer bar stiffness for i-th subproblem

6.3. Optimization results

A single optimal solution (one point of the Pareto set) was obtained after nine iterations of ATC coordination. The obtained target values for the responses at the vehicle level are listed in Table 3. The baseline values are chosen by pre-testing several candidates of initial points of suspension design variables which have relatively good responses. Table 4 summarizes the pairs of target and response values of the K&C curves for the ride comfort objective. We can see that the target and response values converged fully. In the two other subproblems for stability and controllability, the same optimal coefficient values of K&C curves are obtained because the three subproblems share the suspension design variables that generate the K&C curves. Figure 8 shows the K&C curve for left front wheel longitudinal position with wheel travel. The solid line indicates the optimal K&C curve, and the dotted line indicates the K&C curve for the baseline design. Table 5 lists the optimal shared design values at the system level. Superscripts $(\cdot)^{lb}$ and $(\cdot)^{ub}$ indicate variables at their lower and upper bounds, respectively. From these results, we can see that all shared variables have converged fully. While the value differences in Table 3 appear very small, they represent significant differences in the design variable values and in the drivers' expressed "feeling" regarding R&H quality.

Table 3: Targets and responses at the vehicle level

Response	Target value	Baseline value	Final value
Ride comfort	12.0142	12.0180	12.0135
Stability	1.4503	1.5049	1.4947
Controllability	1.0127	1.0082	1.0087

Table 4: Targets and responses at the system level

	Coefficients of K&C curve	Target value from vehicle level	Response value from system level	Deviation between target and response
1st curve (Left toe angle)	Constant c_0	9.743E-03	9.743E-03	0.0%
	1st order coefficient c_1	1.479E-03	1.478E-03	0.0%
	2nd order coefficient c_2	-1.761E-06	-1.767E-06	-0.3%
2nd curve (Right toe angle)	Constant c_0	1.690E-04	1.690E-04	0.0%
	1st order coefficient c_1	1.508E-03	1.508E-03	0.0%
	2nd order coefficient c_2	-2.571E-06	-2.577E-06	-0.2%
3rd curve (Left camber angle)	Constant c_0	-4.234E-03	-4.234E-03	0.0%
	1st order coefficient c_1	-2.299E-02	-2.299E-02	0.0%
	2nd order coefficient c_2	5.994E-05	5.995E-05	0.0%
4th curve (Right camber angle)	Constant c_0	-4.234E-03	-4.234E-03	0.0%
	1st order coefficient c_1	-2.299E-02	-2.299E-02	0.0%
	2nd order coefficient c_2	5.995E-05	5.995E-05	0.0%
5th curve (Left front wheel longitudinal position)	Constant c_0	6.121E-02	6.120E-02	0.0%
	1st order coefficient c_1	5.563E-03	5.558E-03	0.1%
	2nd order coefficient c_2	-2.031E-05	-2.033E-05	-0.1%
6th curve (Right front wheel longitudinal position)	Constant c_0	4.873E-02	4.873E-02	0.0%
	1st order coefficient c_1	5.659E-03	5.654E-03	0.1%
	2nd order coefficient c_2	-2.285E-05	-2.287E-05	-0.1%

Table 5: Optimal shared variables at the system level

(a) Hard point

	LCA front bush			LCA rear bush			Outer tie rod			Knuckle MTG
Axis	x	y	z	x	y	z	x	y	z	z
y_1	-277.4	-378.0^{ub}	-43.7^{ub}	-90.0	-381.6	-44.8	-133.5	-799.5	-66.6	-105.8
y_2	-277.4	-378.0^{ub}	-43.7^{ub}	-90.0	-381.6	-44.8	-133.5	-799.5	-66.6	-105.8
y_3	-277.4	-378.0^{ub}	-43.7^{ub}	-90.0	-381.6	-44.8	-133.5	-799.5	-66.6	-105.8

(b) Bushing stiffness, damper, and stabilizer bar stiffness

	LCA front bush			LCA rear bush			Damper	Stabilizer bar
Axis	Radial	Axial	Conical	Radial	Axial	Conical		
y_1	1.74	1.01	572960	1.59	581.0	572960	0.90	24.93
y_2	1.74	1.01	572960	1.59	581.0	572960	0.90	24.93
y_3	1.74	1.01	572960	1.59	581.0	572960	0.90	24.93

7. Conclusion

We presented a methodology for solving multiobjective optimization problems when an all-in-one approach cannot be used either because of problem size and complexity or because of lack of control over all objectives and the analyses required for their evaluation. The work was motivated by two observations: The first one is that the above mentioned challenges are typical in multidisciplinary design optimization problems. The second one is that solving MO problems using an aggregate objective functions results in problem formulations that are identical to quasi-separable MDO problem formulations. The methodology we proposed uses the extension of analytical target cascading to non-hierarchical formulations. Two examples demonstrated that the non-hierarchical ATC coordination is effective and efficient because it treats subproblem coupling directly without the need for a master problem. The vehicle design problem features a hybrid ATC implementation that also utilizes a hierarchical formulation for coordinating subproblems nested within subproblems; it also demonstrates that ATC can solve large problems (108 variables) efficiently (9 iterations to convergence). A current limitation of the methodology is that non-convex parts of Pareto sets may not be generated as a linear AOF is used, which is a subject for further investigation. It must be noted, however, that this limitation is typical for all AOF-based methods and is not an artifact of the decomposition-based formulation.

8. Acknowledgment
This research was partially supported by Hyundai Motor Company; the authors are grateful for this support. The authors would also like to acknowledge the valuable contributions of Altair Engineering and Hyundai Motor Company in the formulation, modeling, and simulation of the vehicle suspension design example.

9. References

[1] T.W. Athan and P.Y. Papalambros, A Note on Weighted Criteria Methods for Compromise Solutions in Multi-Objective Optimization, *Engineering Optimization*, 27(2), 155-176, 1996.

[2] R.T. Haftka and L.T. Watson, Multidisciplinary Design Optimization with Quasi-separable Subsystems, *Optimization and Engineering*, 6(1), 9-20, 2005.

[3] S. Tosserams, L.F.P. Etman and J.E. Rooda, An Augmented Lagrangian Decomposition Method for Quasi-separable Problems in MDO, *Structural and Multidisciplinary Optimization*, 34(3), 211-227, 2007.

[4] H.M. Kim, *Target cascading in optimal system design*, Ph.D. Dissertation, Mechanical Engineering Dept., University of Michigan, Ann Arbor, MI, 2001.

[5] S. Tosserams, M. Kokkolaras, L.F.P. Etman and J.E. Rooda, A Non-hierarchical Formulation of Analytical Target Cascading, *ASME Journal of Mechanical Design*, 132(5):051002/1-13, May 2010. DOI: 10.1115/1.4001346.

[6] S. Tosserams, L.F.P. Etman, P.Y. Papalambros and J.E. Rooda, An Augmented Lagrangian Relaxation for Analytical Target Cascading Using the Alternating Direction Method of Multipliers, *Structural and Multidisciplinary Optimization*, 31(3), 176-189, 2006.

[7] H.M. Kim, N.F. Michelena, P.Y. Papalambros and T. Jiang, Target Cascading in Optimal System Design, *Journal of Mechanical Design*, 125(3), 474-480, 2003.

[8] MathWorks, *Matlab R2012a*, Available at: http://www.mathworks.com, 2012.

[9] ISO 2631, *Mechanical Vibrationand Shock-Evaluation of Human Exposureto Whole-body Vibration-Part 1: General Requirements*, Int. Standards Organization, 1997.

[10] ISO 13674-1, *Road vehicles - Test method for the quantification of on-centre handling - Part 1: Weave test*, Int. Standards Organization, 2003.

[11] ISO 7401, *Road Vehicles-Lateral Transient Response Test Methods*, Int. Standards Organization, 1988.

[12] Mechanical Simulation, *CarSim Version 8*, Available at: http://www.carsim.com, 2006.

[13] Altair, *MotionSolve Version 11.0*, Available at: http://www.altairhyperworks.com, 2012.

[14] D.O. Kang, S.J. Heo, M.S. Kim, W.C. Choi and I.H. Kim, Robust design optimization of suspension system by using target cascading method, *International Journal of Automotive Technology*, 13 (1), 109-122, 2012.

[15] M. Kokkolaras, L.S. Louca, G.J. Delagrammatikas, N.F. Michelena, Z.S. Filipi, P.Y. Papalambros, J.L. Stein and D.N. Assanis, Simulation-based optimal design of heavy trucks by model-based decomposition: An extensive analytical target cascading case study, *International Journal of Heavy Vehicle Systems*, 11 (3-4), 403-433, 2004.

[16] N. Kang, P.Y. Papalambros, M. Kokkolaras, S. Yoo, W. Na, J. Park and D. Featherman, Optimal Design of Commercial Vehicle Systems Using Analytical Target Cascading, *14th AIAA/ISSMO Multidisciplinary Analysis and Optimization Conference*, Indianapolis, IN, 2012.